Original Article

Three-dimensional evaluation of subclinical extension of extramammary Paget's disease: Visualization of histological border and its comparison to clinical border

Running head: Distributional patterns of Paget cells in extramammary Paget's disease

2646 words, 4 figures, 1 supplemental figure, 2 supplemental tables, 1 supplemental information, and 1 supplemental movie

T. Murata[1,2], T. Honda[1], G. Egawa[1], A. Kitoh[1], T. Dainichi[1], A. Otsuka[1], S. Nakajima[1], S. Kore-eda[3], Y. Kaku[1], S. Nakamizo[1], Y. Endo[1], A. Fujisawa[1], Y. Miyachi[1], and K. Kabashima[1,4,5]

[1]Department of Dermatology, Kyoto University Graduate School of Medicine, Kyoto 606-8507, Japan

[2]Research Fellow of the Japan Society for the Promotion of Science

[3]Tenri Hospital, Tenri, Japan

[4]Singapore Immunology Network (SIgN) and Institute of Medical Biology, Agency for Science, Technology and Research (A*STAR), 8A Biomedical Grove, IMMUNOS Building #3-4, Biopolis, 138648 Singapore

[5]PRESTO, Japan Science and Technology Agency, 4-1-8 Honcho, Kawaguchi, Saitama 332-0012, Japan

Correspondence should be addressed to:
Tetsuya Honda (T.H) and Kenji Kabashima (K.K)
Department of Dermatology, Kyoto University Graduate School of Medicine
54 Shogoin-Kawahara, Sakyo-ku, Kyoto 606-8507, Japan
Tel: +81-75-751-3310, Fax: +81-75-751-4949
E-mail: hontetsu@kuhp.kyoto-u.ac.jp (T.H) and kaba@kuhp.kyoto-u.ac.jp (K.K)

Funding sources: JSPS KAKENHI (JP26-5153) and Agency for Medical Research and Development (16he0902003h0002)
Conflict of interest: none
Key words: extramammary Paget's disease; two-photon microscopy; dermoscopy; subclinical extension

Summary

Background

In extramammary Paget's disease (EMPD), Paget cells are sometimes detected outside the clinical border (subclinical extension). The spreading pattern of Paget cells in subclinical extension, however, remains unclear. In addition, the macroscopic appearances of lesions accompanied by subclinical extension are totally unknown.

Objectives

To characterize the spreading pattern of Paget cells as well as the macroscopic appearance of lesions of EMPD with subclinical extension.

Methods

Nineteen patients with primary anogenital EMPD underwent mapping biopsies and excisional surgeries, then biopsy samples were taken at the periphery of well-demarcated lesions. Samples were transparentized and subjected to whole-mount immunostaining with anti-cytokeratin 7 antibody to label Paget cells. The histological border was evaluated in three dimensions by two-photon microscopy. The shape and location of the histological border were compared with those of the clinical border.

Results

In 21 samples taken at the lesion where subclinical extension was not shown by mapping biopsy, the shape and location of the histological border were almost identical to those of the clinical border. Two samples, however, exhibited small foci of Paget cells outside the clinical border, showing subclinically extended satellite lesions. In the two samples taken at the lesions where subclinical extension was shown by mapping

biopsy, a continuous arrangement of Paget cells extending beyond the clinical border was identified. Subclinically extended Paget cells were detected solely outside hypopigmented patches with erythema.

Conclusions

In EMPD, at least two patterns of subclinical extension exist: continuous and satellite lesions. Subclinical extension might exist preferentially outside hypopigmented patches with erythema.

Introduction

Extramammary Paget's disease (EMPD) is a rare cutaneous malignant tumor that presents as a white-to-erythematous plaque, sometimes accompanied by hyper-/hypo-pigmented patches, typically involving the anogenital area of elderly individuals[1].

To date, several conflicting results have been obtained on the clinical and histological characteristics in EMPD. For example, the local recurrence rates considerably vary according to reports (0 to 60%) even after wide local excision (up to 3 cm)[2–9]. Another controversy is the spreading distance of subclinical extension (the distance at which tumor cells (Paget cells) extend beyond the clinical margin)[1,10,11], which range from several millimeters to several centimeters according to the reports[7,10,12,13]. The multicentric property of EMPD lesions is also a matter of debate. Although such lesions are separated from each other macroscopically, existence of histological connection (thin subclinical extension connecting each lesion) is proposed[14]. Most importantly, the macroscopic appearances of the lesions accompanied by subclinical extension are totally unknown.

One of the major reasons that cause these controversies may be due to our lack of knowledge of the spreading pattern of Paget cells beyond the clinical margin (Fig. 1a). To understand this, a direct comparison of the shape and location between the histological and clinical borders is ideal.

Two-photon microscopy (TPM) is a fluorescence microscope that enables three-dimensional imaging inside biological tissues at a subcellular resolution[15–17]. Although the imaging depth of TPM is not enough to be applied for human skin

disorders[18–23], recently developed methods of tissue-clearing have significantly improved its observational depth by TPM[24–28]. Moreover, some of these methods have significantly improved the efficiency of whole-mount immunohistochemistry (WM-IHC) by increasing the permeability of antibodies into the tissues[27,28]. Therefore, TPM with WM-IHC can visualize the distribution of Paget cells in unsliced specimens.

In this report, we utilized a tissue-clearing method and TPM to visualize Paget cells in unsliced biopsy samples of EMPD. We characterized the spreading pattern of Paget cells in the epidermis, and compared the shape and location between the clinical and histological borders in EMPD.

Materials and methods

Study design

The study was divided in two parts, the newly developed methodology and its clinical implication. In the newly developed methodology part, we assessed the methodology to determine the clinical and histological borders in the same biopsy sample. Nine patients with EMPD and five biopsy samples were observed with dermoscopy and TPM, respectively.

In the clinical implication part, the shape and location of the clinical and histological borders were compared in 23 biopsy samples of EMPD (Fig. 1b).

Patients

This study was approved by an internal review board, and complied with the Helsinki Ethical Principles for Medical Research.

A total of 19 Japanese patients (12 males and 7 females, mean age 70, range 42-80, Supplemental Table 1) undergoing surgical resection of primary anogenital EMPD in the Department of Dermatology of Kyoto University and Tenri Hospital between June 2014 and November 2015 were included in this study with written informed consent. The diagnosis of EMPD was confirmed by histology in all patients.

Clinical characteristics of patients

Clinical findings are summarized in Supplemental Table 1. Of note, hypopigmented patches were observed in 11 cases (58%). All of these patches were located in the

circumferences of the lesions (Supplemental Fig. 1a, arrowheads) and the existence of Paget cells in these patches was confirmed by histology. The existence of hypopigmented patches behind erythematous lesions was assessed by dermoscopy (Supplemental Fig. 1b, asterisks) and diascopy (Supplemental Fig. 1c, d). In three cases (16%), two discrete lesions were found separate from each other in the anogenital area. In two of these three cases, the size of two lesions distinctly differed, and the smaller one consisted only of a hypopigmented patch (Supplemental Fig. 1a, arrow).

Treatment strategy and outcomes

Preoperative mapping biopsy was carried out at spots 1 and 3 cm outside the clinical borders for at least eight directions, as is routinely performed for the management of EMPD in our hospitals. Histological evaluation detected Paget cells in two cases. In each case, Paget cells were detected in one sample at a distance of 1 cm from clinically clear borders (Supplemental Fig. 1e-h, arrows). Surgical lines of excision were defined by connecting inner points of mapping biopsy which were negative for Paget cells. Conventional histopathology revealed one case with positive margin status (Patient number 10), in which case further excision was not performed. The follow-up period ranged 11-29 months (average: 17.2 months) and no local recurrences were detected.

Tissue sampling

After excisional surgeries, one or two samples were taken from each case. All samples were taken at the periphery of well-demarcated lesions. In one of three cases with two

lesions in the anogenital area (Patient number 14), a sample was taken to include both lesions. The size of samples was determined individually so as not to disturb the post-operative histological assessment, and ranged from 1.1 cm × 0.9 cm to 3.8 cm × 1.3 cm.

Tissue-clearing and WM-IHC

Among four representative methods of tissue-clearing, we employed the CUBIC method (Supplemental Table 2) [24–26,28]. The CUBIC method was achieved with slight modification (Supplemental Information)[9]. WM-IHC was achieved with an antibody against cytokeratin 7(CK7), which is specifically expressed in Paget cells of EMPD as well as normal structures of eccrine and apocrine ducts/glands[29–33].

The sensitivity and specificity of WM-IHC were confirmed by observing the treated samples in sections. The signals of CK7 co-existed with tumor cells in hematoxylin-eosin staining, in accordance with previous reports[29–31].

Microscopy, dermoscopy, and i**mage analysis**

Details of devices, settings, and image processing are summarized in Supplemental Information.

Results

Newly developed methodology

In the newly developed methodology part, we assessed the detectability of the clinical and histological borders by dermoscopy and TPM, respectively. Nine patients with EMPD and five biopsy samples were analyzed.

Determination of clinical border by dermoscopy

In agreement with the previous report, EMPD lesions exhibited characteristic features in dermoscopic images, including milky red areas, white structureless areas, gray/brown dots, and gray structureless areas (Supplemental Fig. 1b)[34]. In contrast, none of these characteristic changes on dermoscopic images were observed outside the clinical borders determined by macroscopic observation. Therefore, the clinical borders determined by macroscopic observation were identical to the borders determined by dermoscopy. Of note, pigmentary changes in dermoscopic images were reproducibly obtained in excised samples. In macroscopically ill-demarcated lesions, dermoscopic patterns showed gradual transition and no definite borderlines were delineated. These areas were excluded from subsequent studies.

Determination of histological border by TPM

TPM observation with a tissue-clearing method (Fig. 2a, b) visualized the three-dimensional distribution of Paget cells in unsliced samples of EMPD. In the non-lesional side, weakly CK7-positive cells were detected only at the intraepidermal

sweat ducts, showing coil-like structures (Fig. 2c, d, arrowhead, inset, Supplemental Movie 1). In the lesional side, CK7-positive cells were diffusely located in the lower epidermis (Fig. 2d, lower panel), or in all layers of the epidermis (Fig. 2e, lower panel).

Taken together, three-dimensional TPM analysis was sensitive enough to visualize a single Paget cell, and could visualize the histological borders of Paget cells.

Clinical implication

In the clinical implication part, the shape and location of the clinical borders were compared to those of histological borders in 23 biopsy samples taken from 19 patients as shown in Fig. 1b. We classified the samples in two categories. The category one includes 21 samples in which Paget cells were not proved by preoperative mapping biopsy. The category two includes two samples in which subclinically extended Paget cells were proved by mapping biopsy (Supplemental Table 1). Finally, we evaluated the macroscopic appearances of lesions accompanied by subclinical extension.

Continuous and multicentric/satellite spreading patterns of Paget cells

Firstly, we examined the existence of Paget cells outside the clinical border in category one.

In 18 samples, CK7-positive cells formed a histologically clear border with polygonal shape in TPM images (Fig. 3a-c, red lines). The location and shape of this border were almost identical to those of the clinical border (Fig. 3a-c, yellow lines).

In two samples, small foci of CK7-positive cells were observed outside and in

isolation from the histologically clear border of the main lesion (Fig. 3d-h, arrows). The distance between CK7-positive cells in the small foci and the border of the main lesion was less than 1.4 mm. Since both of these foci were undetectable in dermoscopic images (Fig. 3e), we regarded them as subclinically extended satellite lesions.

In one sample that included two discrete lesions clinically separated from each other, the histological border corresponded to the clinical border in each lesion (Fig. 3i-l and Supplemental Fig. 1a). CK7-positive cells were not detected in the normal appearing skin between the two lesions (Fig. 3i).

To summarize, in most samples (21/23 samples), Paget cells formed a histologically clear border at the edge of the main lesion, which was almost identical to those of the clinical border. This border was sometimes accompanied by the subclinical extension of a small satellite pattern (Fig 3m).

Continuous spreading pattern of Paget cells in subclinical extension

Next, we examined the histological characteristics and horizontal spreading pattern of Paget cells in category two (Fig 3m).

CK7-positive cells spread beyond the clinical border in both cases (Fig. 4a-e). The number of CK7-positive cells and nests decreased markedly at the clinical border (Fig. 4a, e, yellow lines). It is of note that the distribution of Paget cells in subclinically extended lesions was sparse and isolated from each other in the two-dimensional analysis of histology (Fig. 4f-k, arrows). However, three-dimensional TPM images revealed the proximity of each CK7-positive cell in subclinically extended lesions (Fig.

4d, inset), forming histologically clear borders (Fig. 4a, d, red line). The gap between the histological and clinical borders was within 10 mm (Fig. 4c, green area). The histological borders of the subclinical extension (Fig. 4c, red line) were not finger-like or highly irregular when compared to the clinical borders (Fig. 4c, yellow line).

Taken together, a three-dimensional TPM analysis visualized a continuous pattern of subclinical extension, in which the regularity of the histological border and the clinical border was almost comparable.

Characteristics of macroscopic appearance of clinical borders with subclinical extension

Finally, we evaluated the clinical appearances of lesions with subclinical extension. Conventionally, the macroscopic appearances of EMPD lesions have been described as pigmented, erythema, hypopigmented and hypopigmented patches with erythema. However, as previously mentioned (see "newly developed methodology" section), erythematous lesions were consistently accompanied by hypo- or hyper-pigmentation. Therefore, we divided the appearances of the sampling area into four groups in terms of pigmentary changes and existence of erythema as follows (Supplemental Table 1).

Subclinical extensions, including both satellite and continuous lesions, were found outside hypopigmented patches with erythema (4/13 samples, Supplemental Fig. 1e-h), but not outside hypopigmented patches (0/5 samples), hyperpigmented patches (0/3 samples), or hyperpigmented patches with erythema (0/2 samples).

Discussion

In this study, we visualized Paget cells of EMPD in three-dimensions, and assessed the spreading pattern of Paget cells. To our knowledge, this is the first application of TPM observation of human tissues in combination with tissue-clearing method to address clinical questions in human diseases.

It has long been unclear how Paget cells spread at the periphery of the lesions. Several reports have suggested a highly irregular histological border in subclinical extended lesions compared to the clinical border[10,11,14,35]. It remains unclear, however, whether this is the major distributional pattern.

In all of the samples examined in this study, a histologically clear border of Paget cells was visualized at the edge of the main lesion. The shape of this border was polygonal and comparable to that of clinical border even in lesions with continuous pattern of subclinical extension. These results indicate that a continuous distribution of Paget cells forming a polygonal borderline is the major spreading pattern in EMPD. At present, we cannot exclude the existence of highly irregular borderlines[10,14], because our observation was restricted to only a portion of well-demarcated lesions from 19 cases. Our results, nevertheless, suggest that a highly irregular spreading pattern is not as common as previously advocated[10,14].

The existence of histologically separated lesions in the anogenital area has also been a matter of debate. In the present study, three-dimensional analysis confirmed that the lesions were not always connected by thin extensions of Paget cells. Unexpectedly, small satellite lesions of subclinical extension were found only in the vicinity of the

main lesions. These results suggest that there might be a minor but characteristic spreading pattern in EMPD; Paget cells might migrate in the epidermis from the border of the main lesion, and proliferate as a separate lesion. Although it is unclear whether clinically separated lesions are derived from migrated cells or develop multicentrically, our results support the existence of histologically separated lesions in EMPD and indicate a unique migratory property of Paget cells.

The number of Paget cells clearly changed at the clinical border, indicating a close relationship between the number of Paget cells and the clinical appearances. As previously reported, Paget cells in subclinical extension are located mainly in the lower epidermis, where Paget cells are considered to proliferate[36–38]. Therefore, we speculate that subclinical extension is an early developing lesion, in which Paget cells expand mainly outward, and do not markedly increase in number. Intriguingly, all four subclinical extensions were located outside the clinical borders of hypopigmented patches with erythema. Although we could not perform statistical analysis with this small number of samples, this clinical appearance might indicate a lesion with Paget cells expanding outward, giving rise to a subclinical extension. Thus, it might be beneficial to manage hypopigmented patches with erythema more carefully than other types of lesions, for example, by performing thorough mapping biopsy or extensive post-operative assessment of the histological margin.

Subclinical extension larger than 1 cm was detected in only two areas in 2 of the 19 cases examined. This low rate of clinically significant subclinical extension is similar to reports from Japan by Murata and Kumano (0/137 sections in 46 cases)[7] and Kato et al.

(8/86 biopsy sites in 17 cases)[39], which were shown to be comparable between well- and ill-demarcated lesions[39]. In contrast, Gunn and Gallager[10] reported a broad extension of Paget cells surrounding the whole lesion (4/4 cases), in accordance with the report by Pitman et al. (>3 cm, 47% of biopsy sites)[12]. Furthermore, reports on Mohs microscopic surgery have shown the necessity of plural Mohs stages (75-100% of cases)[3,5,36,40,41].

What caused this discrepancy? A possible explanation might be the visibility of hypopigmented lesions in each study. In our study, all the patients were Asian, whereas most of studies showing a high rate of subclinical extension were analyzing Caucasian patients[2,3,5,10,12,13,36,40]. Hypopigmented lesions were reported to be common in Asian patients with EMPD[8,34,42]. In contrast, to the best of our knowledge, hypopigmented lesions in Caucasian patients have not been described. Considering that the detection of depigmented lesions surrounding the erythematous plaque is sometimes very difficult even in the colored skin of Asians[7], tumor cells might not provoke visible hypopigmentation in the skin of Caucasians, resulting in the apparently wide existence of subclinical extensions, even though we could not draw a definite conclusion due to the limited number of cases in this study. Although Mohs microscopic surgeries have been applied successfully in Western countries to treat EMPD (local recurrence rate 12.2%)[2], further lower recurrence rates (0-10%) were reported from Asian countries even with an excisional margin of 1 cm[7–9]. In addition, in two of three cases with multiple lesions in this study, one of these lesions consisted only of hypopigmentation. These lesions might be totally invisible in Caucasians, contributing to the relatively high local recurrence rate even after Mohs micrographic surgeries[2]. Such

hypopigmented lesions might become visible, if the pigmentation of normal skin surrounding the lesions could be enhanced by some interventions, such as ultraviolet radiation.

In summary, three-dimensional histological analysis shed light on the spreading pattern of Paget cells in EMPD. Further analysis would contribute to the optimization of surgical management in EMPD.

References

1 Goldsmith LA, Fitzpatrick TB. Fitzpatrick's dermatology in general medicine. New York, McGraw-Hill Medical, 2012.

2 Bae JM, Choi YY, Kim H, *et al.* Mohs micrographic surgery for extramammary Paget disease: a pooled analysis of individual patient data. *J Am Acad Dermatol* 2013; **68**:632–7.

3 Hendi A, Brodland DG, Zitelli JA. Extramammary Paget's disease: Surgical treatment with Mohs micrographic surgery. *J Am Acad Dermatol* 2004; **51**:767–73.

4 Marchesa P, Fazio VW, Oliart S, *et al.* Long-term outcome of patients with perianal Paget's disease. *Ann Surg Oncol* 1997; **4**:475–80.

5 O'Connor WJ, Lim KK, Zalla MJ, *et al.* Comparison of Mohs Micrographic Surgery and Wide Excision for Extramammary Paget's Disease. *Dermatol Surg* 2003; **29**:723–7.

6 Coldiron BM, Goldsmith BA, Robinson JK. Surgical treatment of extramammary paget's disease. A report of six cases and a reexamination of mohs micrographic surgery compared with conventional surgical excision. *Cancer* 1991; **67**:933–8.

7 Murata Y, Kumano K. Extramammary Paget's disease of the genitalia with clinically clear margins can be adequately resected with 1 cm margin. *Eur J Dermatol* 2005; **15**:168–70.

8 Hatta N, Yamada M, Hirano T, *et al.* Extramammary Paget's disease: treatment, prognostic factors and outcome in 76 patients. *Br J Dermatol* 2008; **158**:313–8.

9 Wang Z, Lu M, Dong G-Q, *et al.* Penile and Scrotal Paget's disease: 130 Chinese patients with long-term follow-up. *BJU Int* 2008; **102**:485–8.

10 Gunn RA, Gallager HS. Vulvar Paget's disease. A topographic study. *Cancer* 1980; **46**:590–4.

11 Lam C, Funaro D. Extramammary Paget's Disease: Summary of Current Knowledge. *Dermatol Clin* 2010; **28**:807–26.

12 Pitman GH, McCarthy JG, Perzin KH, Herter FP. Extramammary Paget's

disease. *Plast Reconstr Surg* 1982; **69**:238–44.

13 Appert DL, Otley CC, Phillips PK, Roenigk RK. Role of Multiple Scouting Biopsies before Mohs Micrographic Surgery for Extramammary Paget's Disease. *Dermatol Surg* 2005; **31**:1417–22.

14 Hendi A, Perdikis G, Snow JL. Unifocality of extramammary Paget disease. *J Am Acad Dermatol* 2008; **59**:811–3.

15 Natsuaki Y, Egawa G, Nakamizo S, *et al.* Perivascular leukocyte clusters are essential for efficient activation of effector T cells in the skin. *Nat Immunol* 2014; **15**:1064–9.

16 Egawa G, Nakamizo S, Natsuaki Y, *et al.* Intravital analysis of vascular permeability in mice using two-photon microscopy. *Sci Rep* 2013; **3**:1932.

17 Kabashima K, Egawa G. Intravital multiphoton imaging of cutaneous immune responses. *J Invest Dermatol* 2014; **134**:2680–4.

18 Murata T, Honda T, Egawa G, *et al.* Epicutaneous detection of transepidermally eliminated collagen by multiphoton microscopy: A possible non-invasive diagnosis method for acquired reactive perforating dermatosis. *J Dermatol Sci*; **76**:158–60.

19 Murata T, Honda T, Miyachi Y, Kabashima K. Morphological character of pseudoxanthoma elasticum observed by multiphoton microscopy. *J Dermatol Sci* 2013; **72**:199–201.

20 Tong PL, Qin J, Cooper CL, *et al.* A quantitative approach to histopathological dissection of elastin-related disorders using multiphoton microscopy. *Br J Dermatol* 2013; **169**:869–79.

21 Dimitrow E, Ziemer M, Koehler MJ, *et al.* Sensitivity and Specificity of Multiphoton Laser Tomography for In Vivo and Ex Vivo Diagnosis of Malignant Melanoma. *J Invest Dermatol* 2009; **129**:1752–8.

22 Heuke S, Vogler N, Meyer T, *et al.* Multimodal mapping of human skin. *Br J Dermatol* 2013; **169**:794–803.

23 Chen G, Chen J, Zhuo S, *et al.* Nonlinear spectral imaging of human hypertrophic scar based on two-photon excited fluorescence and second-harmonic generation. *Br J Dermatol* 2009; **161**:48–55.

24 Hama H, Kurokawa H, Kawano H, *et al.* Scale: a chemical approach for fluorescence imaging and reconstruction of transparent mouse brain. *Nat Neurosci*

2011; **14**:1481–8.
25 Kuwajima T, Sitko AA, Bhansali P, *et al.* ClearT: a detergent- and solvent-free clearing method for neuronal and non-neuronal tissue. *Development* 2013; **140**:1364–8.
26 Ke M-T, Fujimoto S, Imai T. SeeDB: a simple and morphology-preserving optical clearing agent for neuronal circuit reconstruction. *Nat Neurosci* 2013; **16**:1154–61.
27 Chung K, Wallace J, Kim S-Y, *et al.* Structural and molecular interrogation of intact biological systems. *Nature* 2013; **497**:332–7.
28 Susaki EA, Tainaka K, Perrin D, *et al.* Whole-brain imaging with single-cell resolution using chemical cocktails and computational analysis. *Cell* 2014; **157**:726–39.
29 Smith KJ, Tuur S, Corvette D, *et al.* Cytokeratin 7 staining in mammary and extramammary Paget's disease. *Mod Pathol* 1997; **10**:1069–74.
30 Battles OE, Page DL, Johnson JE. Cytokeratins, CEA, and mucin histochemistry in the diagnosis and characterization of extramammary Paget's disease. *Am J Clin Pathol* 1997; **108**:6–12.
31 Ohnishi T, Watanabe S. The use of cytokeratins 7 and 20 in the diagnosis of primary and secondary extramammary Paget's disease. *Br J Dermatol* 2000; **142**:243–7.
32 Osamu Y, Masanori H, Hiroshi Y, *et al.* Cytokeratin expression of apocrine and eccrine poromaswith special reference to its expression in cuticular cells. *J Cutan Pathol* 2000; **27**:367–73.
33 Toshihiro T, Yozo M. On the Validity of Skin Biopsies of Normal-Looking Axilla in Patients with Genital Extramammary Paget's Disease. *Jpn J Dermatol* 2013; **123**:2257–61.
34 Mun J-H, Park S-M, Kim G-W, *et al.* Clinical and dermoscopic characteristics of extramammary Paget's disease: a study of 35 cases. *Br J Dermatol* 2015; **174**:1104–7.
35 Zollo JD, Zeitouni NC. The Roswell Park Cancer Institute experience with extramammary Paget's disease. *Br J Dermatol* 2000; **142**:59–65.
36 Mohs FE, Blanchard L. MIcroscopically controlled surgery for extramammary paget's disease. *Arch Dermatol* 1979; **115**:706–8.
37 Kakinuma H, Iwasawa U, Kurakata N, Suzuki H. A case of extramammary Paget's disease with depigmented macules as the sole manifestation. *Br J Dermatol*

1994; **130**:102–5.
38 Pierard-Franchimont C, Pierard GE. Replication of Paget cells in mammary and extramammary Paget's disease. *Br J Dermatol* 1984; **111**:69–74.
39 Kato T, Fujimoto N, Fujii N, Tanaka T. Mapping biopsy with punch biopsies to determine surgical margin in extramammary Paget's disease. *J Dermatol* 2013; **40**:968–72.
40 Boehringer A, Leiter U, Metzler G, *et al.* Extramammary Paget's disease: extended subclinical growth detected using three-dimensional histology in routine paraffin procedure and course of the disease. *Dermatol Surg* 2011; **37**:1417–26.
41 Lee K-Y, Roh MR, Chung WG, Chung KY. Comparison of Mohs Micrographic Surgery and Wide Excision for Extramammary Paget's Disease: Korean Experience. *Dermatol Surg* 2009; **35**:34–40.
42 Yang C-C, Lee JY-Y, Wong T-W. Depigmented extramammary Paget's disease. *Br J Dermatol* 2004; **151**:1049–53.

Figure Legends

Figure 1: Hypotheses and study design

(a) Three hypotheses of spreading of Paget cells beyond clinical margin. Continuous pattern: Paget cells form a histological border with ordinary shape, which locates significantly outside a clinical border. Highly irregular pattern: Paget cells form a histological border with highly irregular shape compared to a histological border. Multicentric/satellite pattern: Paget cells form separate foci outside a clinical border, which suggest a multicentric occurrence of lesions or skipping progression at the periphery of lesions. (b) Study design. To verify these hypotheses, the histological and clinical borders were defined in two-photon microscopy (TPM) and dermoscopic images, respectively. These images were merged in order to compare the shape and location of these borders.

Figure 2: Determination of histological border by TPM

(a, b) Transparentization of a biopsy sample of Patient 04. (a) Before and (b) after tissue-clearing. (c-e) Visualization of Paget cells (cytokeratin 7(CK7): green signal) by TPM. (c) A representative image of the whole sample of Patient 01, including normal (left) and lesional (right) areas. Normal area is visualized by second-harmonic generation of dermal collagen fibers (blue signal). (d) Magnified image of the edge of the lesion at the white rectangle in (c). Upper panel: three-dimensional view. Lower panel: vertical view. Arrows: Paget cells visualized at a resolution of the single-cell level. Arrowhead: weakly CK7-positive cells at the intraepidermal sweat ducts. White

line: the surface of the epidermis. White dashed line: dermo-epidermal junction. Inset: Magnified three-dimensional image at the arrowhead, showing a coil-like structure of intraepidermal sweat ducts. (e) Magnified image of the inner area of the lesion at the cyan rectangle in (c). Upper panel: three-dimensional view. Lower panel: vertical view. Arrows: tumor nests. Scale bars: (a, b) 10 mm, (c) 5 mm, (d, e) 100 μm, inset of (d) 50 μm.

Figure 3: Continuous and multicentric/satellite spreading patterns of Paget cells

(a-l) Three representative samples in the category one, showing different spreading patterns of Paget cells. Red lines: histological borders. Yellow lines: clinical borders.

(a-c) A sample without subclinical extension in Patient 01. (a) TPM image. Diffusely distributed CK7-positive cells (Paget cells: green signal). Blue signal: dermal collagen fibers. (b) Dermoscopic image. Arrow: faint reticular pattern. Arrowhead: hyperpigmented area with gray/brown dots and negative network patterns. (c) Merged image. (d-h) A sample with a focus of CK7-positive cells in Patient 17. (d) TPM image. Arrow: the focus of CK7-positive cells. (e) Dermoscopic image. Arrowhead: Faint reticular pattern in the area corresponding with the focus of CK7-positive cells. (f) Merged image. Green dots: CK7-positive cells of the focus. (g, h) Magnified images at the rectangle in (d). (g) Three-dimensional view. Arrows: CK7-positive cells sparsely distributed as a circular focus. (h) Lower panel: vertical view. (i-l) A sample with multiple macroscopic lesions in Patient 14. (i) TPM image. Arrow: CK7-positive cells in the separate lesion. Arrowhead: CK7-positive cells in the main lesion. (j)

Dermoscopic image. Asterisks: scars of pre-operative biopsy. (k) Merged image. Green area indicates the distribution of CK7-positive cells in the separate lesion. (l) Macroscopic image. Arrow: the smaller lesion. Arrowhead: the main lesion with mild hypopigmentation. White line: the sampling area. Scale bars: (a-f, i-k) 1 mm, (g, h) 500 μm.

(m) Summary of results in the comparison between clinical and histological borders.

Figure 4: Continuous spreading pattern of Paget cells in subclinical extension

A representative sample of Patient 09 in category two: samples with subclinical extension shown by mapping biopsy. Red lines: histological borders. Yellow lines: clinical borders. (a) TPM image showing an extension of CK7-positive cells (Paget cells: green signal) beyond the clinical border. Note the difference in the intensity of green signal between inside and outside the clinical border. Arrow: acanthotic area. Blue signal: dermal collagen fibers. (b) Dermoscopic image. Arrow: faint reticular pattern in areas with CK7-positive cells. Arrowhead: white structureless area. Asterisk: gray/brown dots. (c) Merged image. Green area indicates the subclinical extension. (d, e) Magnified images at the white and cyan rectangles in (a), respectively. Inset: further magnified image of CK7-positive cells in (d). Arrows: CK7-positive single cells. Arrowheads: tumor nests. (f-k) Histological images at normal (f, i), subclinically extended (g, j), and clinically lesional areas (h, k). (f-h) Hematoxylin and eosin staining. (i-k) Immunostaining with CK7. Arrows and arrowheads: Paget cells. Scale bars: (a-e) 1 mm, (f-k): 100 μm.

Supplemental Figure 1: Representative macroscopic appearances of EMPD and determination of clinical border by dermoscopy

Four representative cases with anogenital extramammary Paget's disease (EMPD). (a) Multiple lesions of EMPD in the anogenital area of Patient 14. Arrow: separated lesion. Arrowheads: hypopigmented lesions. (b) Dermoscopic image of the clinical border between normal (upper left) and lesional areas (lower right) at the rectangle in (a). Arrows: clinical border noted by black pen on inspection. Black arrowhead: faint reticular pattern. Red arrowheads: gray/brown dots. Asterisks: erythematous areas on hypopigmentation (milky red appearance). (c, d) Hypopigmentation behind an erythematous lesion in Patient 13. (c) Without and (d) with diascopy. Arrow: hypopigmentation revealed by diascopy. (e-h) Two cases with subclinical extension that was detected by mapping biopsy. (e) A lesion with marked pigmentary changes surrounded by hypopigmented erythema in Patient 09. (f) Magnified image of clinical border at the rectangle in (e). Yellow line: clinical border. Arrow: mapping biopsy site. White dashed line: ill-demarcated lesion. (g) A hypopigmented patch with erythema in Patient 11. (h) Magnified image of the clinical border at the rectangle in (g). Yellow line: clinical border. Arrow: mapping biopsy site. Arrowhead: physiological pigmentation at the perianal region. Scale bar: 100 μm.

Supplemental Movie 1

A representative movie of two-photon microscopy, showing the distribution of CK7-positive cells (Paget cells: green signal) in the sample of Patient 01. Blue signal: second-harmonic generation of collagen. Red signal: autofluorescence of hair shafts.

Supplemental Table 1: Clinical characteristics, histological findings, and results of the analysis

			Skin lesions of extramammary Paget's disease						Histological findings						Lesional type of tissue sampling				Results		Follow-up period (Month)
Patient number	Age	Sex	Area of lesion	Hypo-pigmentation	Hyper-pigmentation	Erythema	Multiple lesions	Ill-demarcated lesion	SE detected by mapping biopsy	Positive margin status	Dermal invasion#	Lymph vessel invasion	Regional lymph node metastasis	Distant metastasis	Number of samples	Area	Erythema	Pigmentary change	Continuous type of SE	Satellite type of SE	
01	76	M	groin, penile shaft, scrotum	-	+	+	-	-	-	-	P	-	-	-	1	groin	-	hyper	-	-	29
02	67	M	penile shaft, scrotum	-	-	+	-	-	-	-	P	-	-	-	1	scrotum	+	hypo	-	-	26
03	79	F	groin, labia minora	-	+	+	-	-	-	-	-	-	-	-	1	groin	-	hyper	-	-	25
04	64	M	groin, penile shaft, scrotum	+	-	+	+	-	-	-	R	-	+	-	2	groin	-	hypo	-	-	20
																groin	-	hypo	-	-	
05	65	M	penile shaft, scrotum	+	-	+	-	+	-	-	R	-	-	-	1	scrotum	+	hypo	-	-	16
06	80	M	penile shaft, scrotum	+	-	+	-	-	-	-	R	+	+	-	2	scrotum	-	hypo	-	-	14
																scrotum	+	hypo	-	-	
07	77	F	vaginal vestibule, perineum, anus	-	-	+	-	+	-	-	P	-	-	-	1	perineum	+	hypo	-	-	14
08	48	F	labia majora, labia minora	-	-	+	-	+	-	-	-	-	-	-	1	labia majora	+	hypo	-	-	13
09	67	M	groin, scrotum	+	+	+	+	+	+	-	-	-	-	-	1	groin	+	hypo	+	-	17
10	65	F	groin, labia majora, labia minora, perineum	+	+	+	-	+	-	+	-	-	-	-	2	perineum	-	hypo	-	-	12
																labia majora	+	hypo	-	-	
11	66	F	groin, labia majora, labia minora, perineum	-	-	+	-	+	+	-	-	-	-	-	2	perineum	+	hypo	+	-	12
																groin	-	hyper	-	-	
12	79	M	groin, scrotum	+	-	+	-	+	-	-	-	-	-	-	1	groin	+	hypo	-	-	12
13	75	M	penile shaft, scrotum	+	+	+	-	+	-	-	P	-	-	-	1	scrotum	+	hypo	-	-	12
14	42	F	mons pubis, labia majora, groin	+	+	+	+	+	-	-	R	-	-	-	1	mons pubis	-	hypo	-	-	11
15	57	M	penile shaft, scrotum	+	+	+	-	-	-	-	P	-	-	-	1	scrotum	+	hyper	-	-	15
16	89	M	scrotum, perineum	+	-	+	-	-	-	-	R	-	+	+	1	scrotum	+	hypo	-	+	20
17	86	M	scrotum	-	-	+	-	-	-	-	R	-	-	-	1	scrotum	+	hypo	-	+	19
18	77	F	labia majora	-	-	+	-	-	-	-	S	+	+	+	1	labia majora	+	hyper	-	-	15
19	64	M	penile shaft, scrotum	+	-	+	-	+	-	-	-	-	-	-	1	scrotum	+	hypo	-	-	25
Total (%)	69.6*	M=12 F=7		11 (57.9)	7 (36.8)	19 (100)	3 (15.8)	10 (52.6)	2 (10.5)	1 (5.3)	12 (63.2)	2 (10.5)	4 (21.1)	2 (10.5)	23 samples	hypopigmented P/P*: 5 hyperpigmented P/P*: 3 erythematous hypopigmented P/P*: 13 rythematous hyperpigmented P/P*: 2			2 (8.7)	2 (8.7)	17.2*

*average, M: male, F: female, hyper: hyperpigmentation, hypo: hypopigmentation, SE: subclinical extension, *Patches/plaques #P: papillary dermis, R: reticular dermis, S: subcutis

Supplemental Table 2: Characteristics of tissue-clearing methods applied for human skin

Sample type	Evaluation		Methods of tissue-clearing			
			Sca/e A2	ClearT	SeeDB	CUBIC
Healthy human skin	Time for transparentization		Half year	Not transparentized	2 weeks	1 week
	Second-harmonic generation of collagen		Disappear	NA	Preserved	Preserved
	Tissue volume		Expanded		Slightly shrinked	No change
	Time for whole-mount immunostaining	Dermis	NA		1-2 weeks	Several days
		Epidermis	NA		2-4 weeks*	1 week*
Extramammary Paget's disease			NA		Not stained	1 week

NA: not assessed

*Assessed with anti-CD1a antibody to stain intraepidermal Langerhans cells

Figure 1

(a) Hypotheses for spreading patterns of Paget cells in subclinical extension

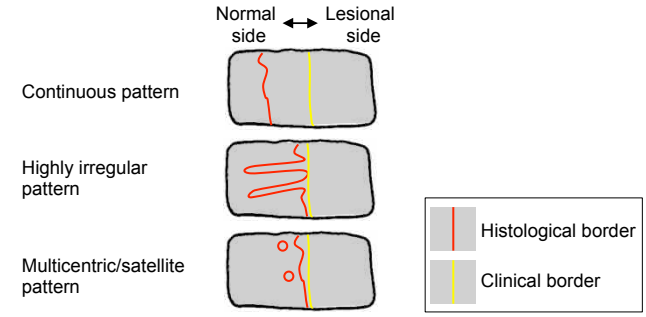

(b) Study design

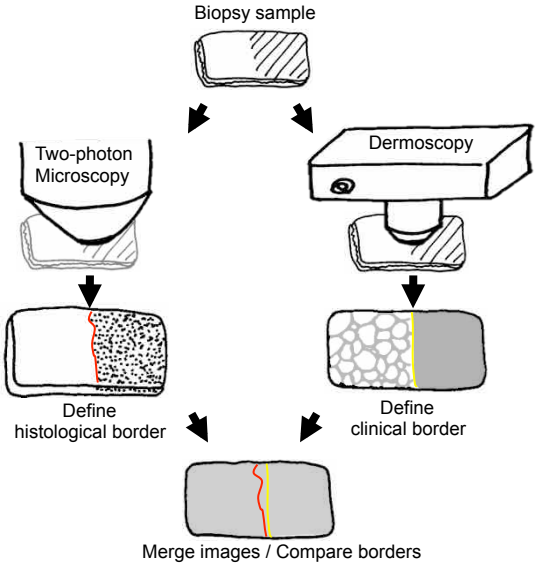

Figure 2

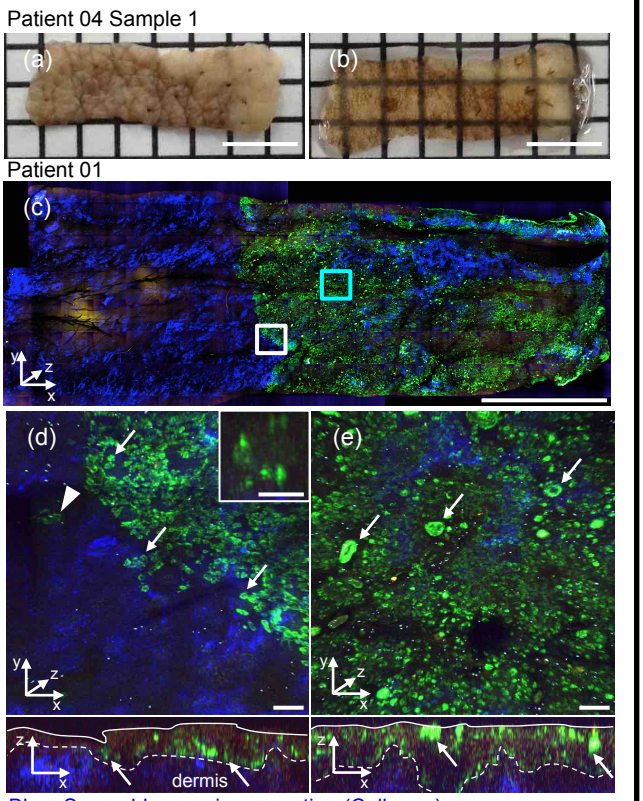
Patient 04 Sample 1
(a)
(b)
Patient 01
(c)
(d)
(e)
dermis
Blue: Second-harmonic generation (Collagen)
Green: Cytokeratin 7 Red: Autofluorescence

Figure 3

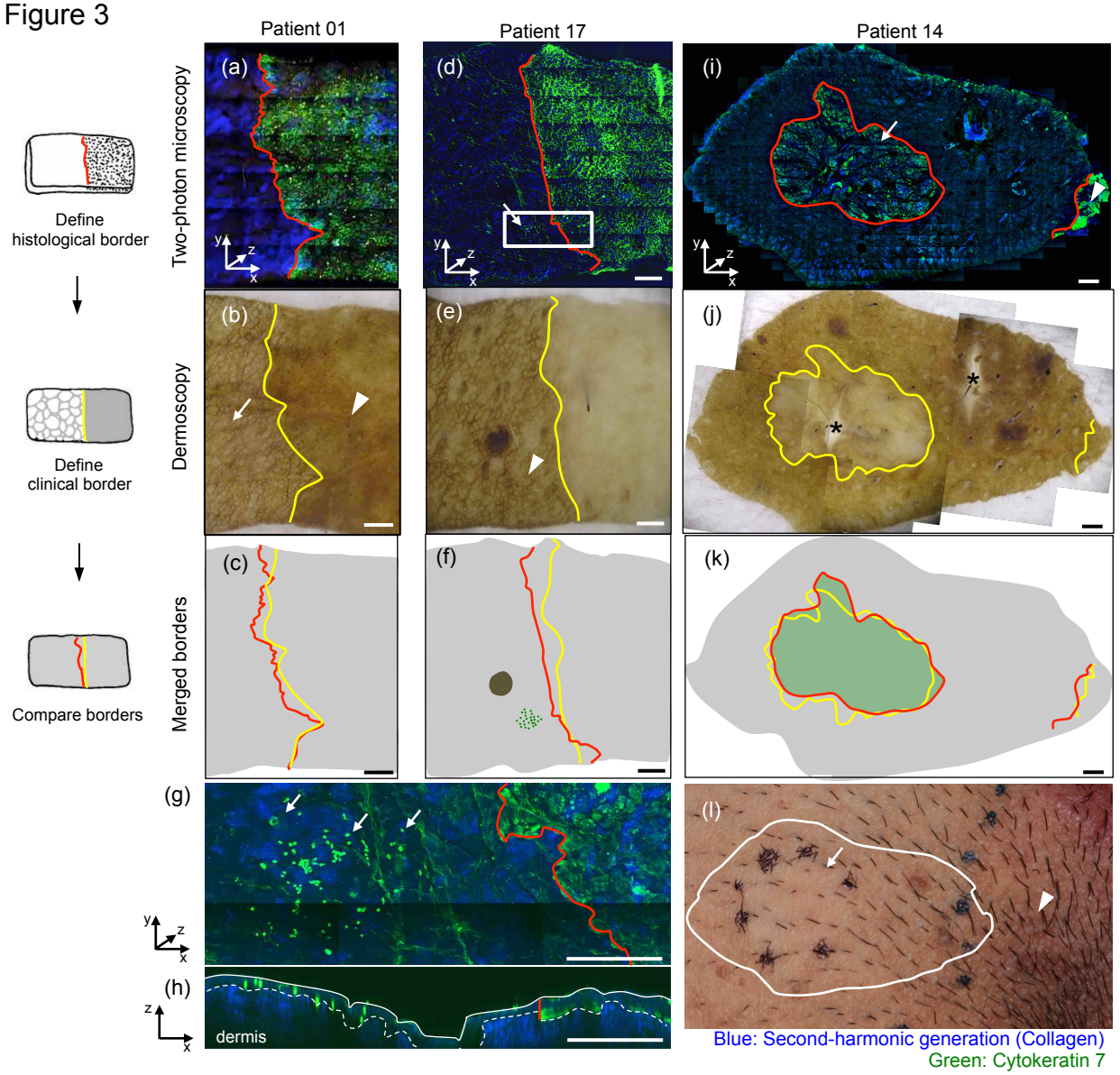

(m)

23 samples

Category 1
21 samples
(subclinical extension was not proved by mapping biopsy)
- 18 samples: Continuous pattern without subclinical extension
- 2 samples: Satellite pattern of subclinical extension
- 1 sample: Continuous pattern without subclinical extension in clinically multiple lesions

Category 2
2 samples
(subclinical extension was proved by mapping biopsy)
- 2 samples: Continuous pattern of subclinical extension

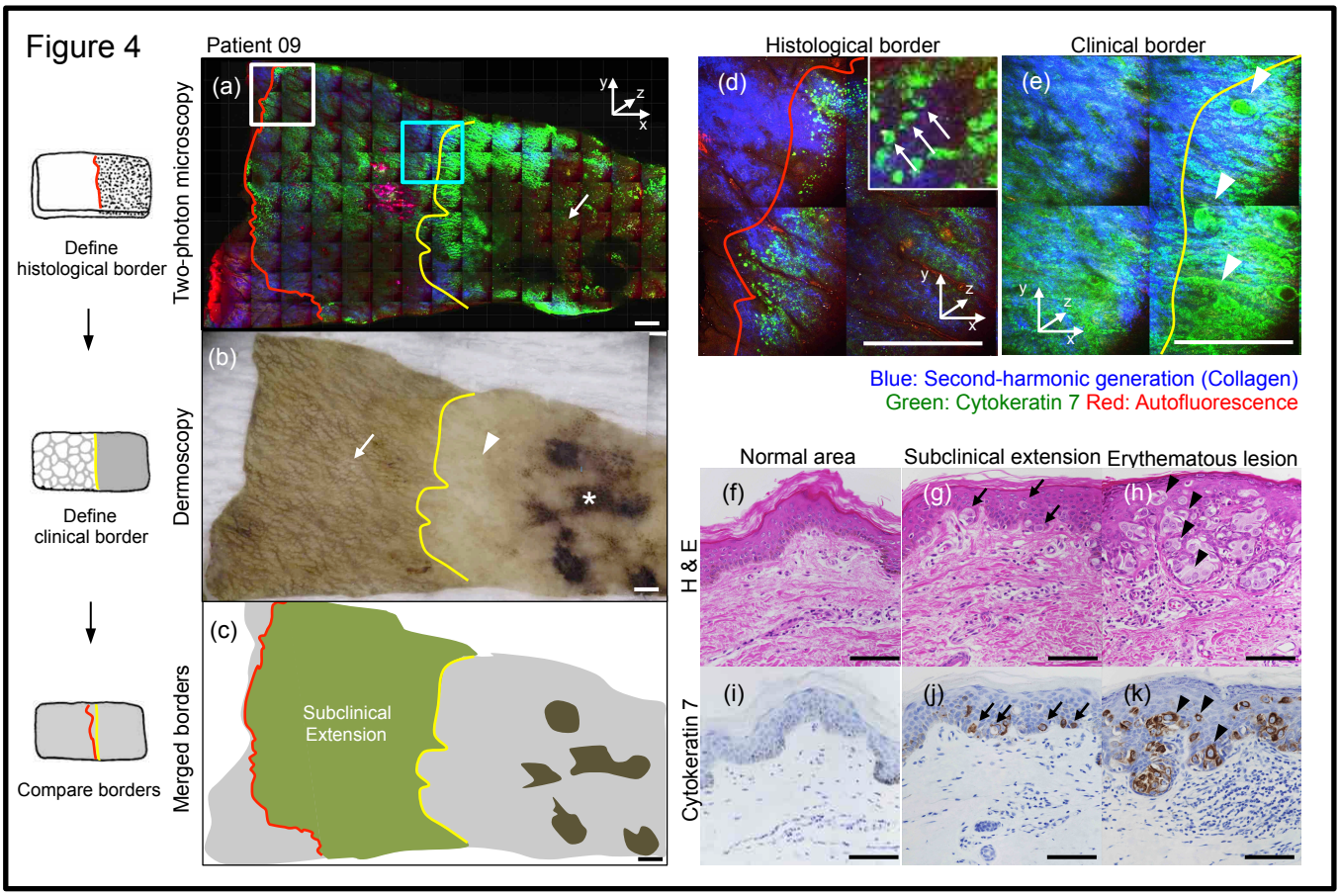
Figure 4
Patient 09
Define histological border
Define clinical border
Compare borders
Two-photon microscopy
Dermoscopy
Merged borders
(a)
(b)
(c)
Subclinical Extension
Histological border
Clinical border
(d)
(e)
Blue: Second-harmonic generation (Collagen)
Green: Cytokeratin 7 Red: Autofluorescence
Normal area
Subclinical extension
Erythematous lesion
H & E
Cytokeratin 7
(f)
(g)
(h)
(i)
(j)
(k)

Supplemental Figure 1

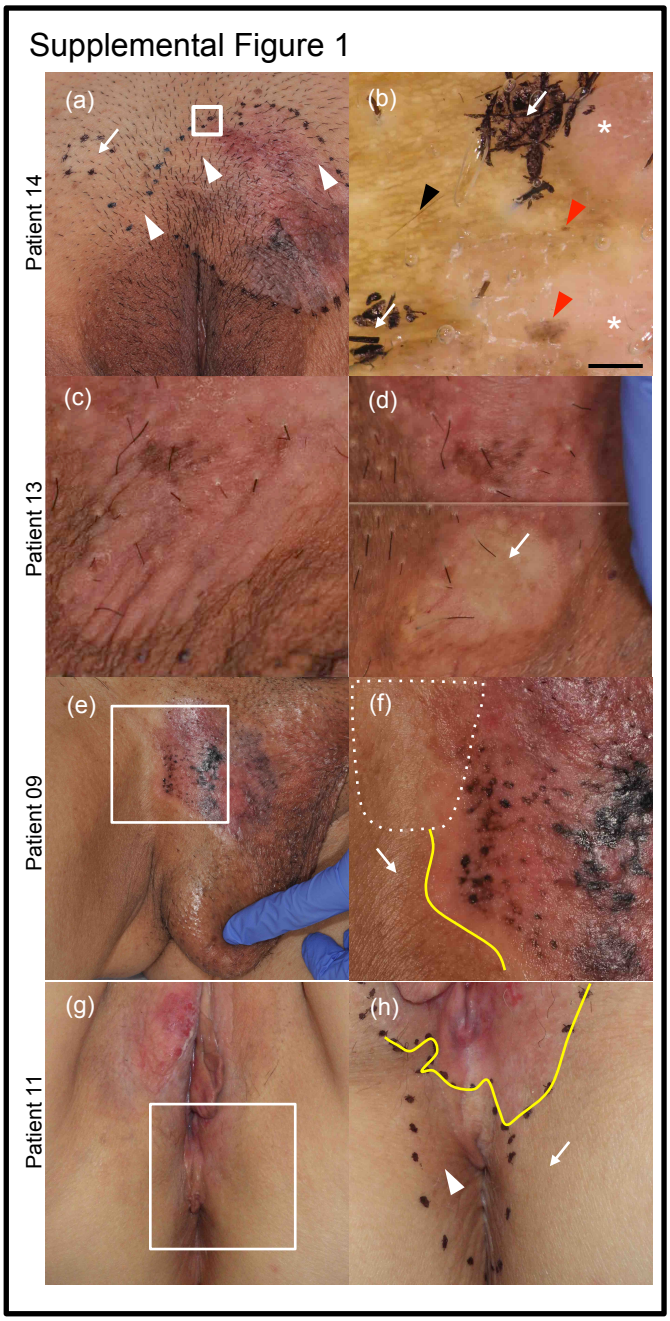

Supplemental Information

Modified CUBIC protocol with whole-mount immunohistochemistry for human skin samples

Biopsy samples of EMPD lesions were fixed with 4% paraformaldehyde at 4ºC over night. Then, adipose tissues were removed with surgical scissors, and immersed in Sca/eCUBIC-1 solution for 3 to 7 days at 4ºC, considering the thickness of samples. After washing with phosphate-buffered saline (PBS), samples were subjected to immunostaining with a primary antibody of monoclonal mouse anti-human cytokeratin 7 (CK7) (clone: OV-TL 12/30, Dako, Carpinteria, USA) and the Alexa Fluor 488 or 594 conjugated secondary antibody of polyclonal donkey anti-mouse IgG (Abcam, Cambridge, UK) at 4°C for 1 week, respectively. The stained samples were then washed with PBS and immersed in Sca/eCUBIC-2 for 24 h at room temperature.

Microscopy

Samples were imaged by TPM, FV1000MPE-IX81 (Olympus, Tokyo, Japan) combined with a MaiTai DeepSee HP-OL laser (Spectra-Physics, San José, USA) at an excitation wavelength of 780 or 990 nm. Second-harmonic generation of collagen and fluorescence of Alexa 488 were detected through 460 to 500 nm and 520 to 560 nm band pass filters, respectively. Fluorescence of Alexa 594, autofluorescence of elastic fibers, hair shafts, and crusts were detected through a 575 to 630 nm band pass filter.

All of the samples were imaged through a 10x objective lens (UPLSAPO, NA=0.4, WD = 3.1 mm, Olympus) from the surface side of the skin down to 350 to 500 μm with intervals of 5 to 10 μm.

Dermoscopy

Dermoscopic pictures were taken with a non-polarized contact-type dermoscopy, Derma 9500 (DMI, Inc., Yokohama, Japan), using echo gel. Since the defatting and tissue-clearing procedures result in transformation of samples, we washed the samples with PBS to make them opaque again and dermoscopic images were then obtained.

Image analysis

Three-dimensional images of TPM were reconstructed with Imaris software version 7.2.1 (Bitplane, Zurich, Switzerland). TPM images were merged with dermoscopic images using ImageJ version 1.45s (NIH, Bethesda, USA).